

Biomimetic vibrissal sensing for robots

Martin J. Pearson, Ben Mitchinson, J. Charles Sullivan, Anthony G. Pipe and Tony J. Prescott

Phil. Trans. R. Soc. B 2011 **366**, 3085-3096

doi: 10.1098/rstb.2011.0164

Supplementary data

["Data Supplement"](#)

<http://rstb.royalsocietypublishing.org/content/suppl/2011/09/13/366.1581.3085.DC1.html>

References

[This article cites 43 articles, 17 of which can be accessed free](#)

<http://rstb.royalsocietypublishing.org/content/366/1581/3085.full.html#ref-list-1>

[Article cited in:](#)

<http://rstb.royalsocietypublishing.org/content/366/1581/3085.full.html#related-urls>

Email alerting service

Receive free email alerts when new articles cite this article - sign up in the box at the top right-hand corner of the article or click [here](#)

To subscribe to *Phil. Trans. R. Soc. B* go to: <http://rstb.royalsocietypublishing.org/subscriptions>

Review

Biomimetic vibrissal sensing for robots

Martin J. Pearson^{1,*}, Ben Mitchinson², J. Charles Sullivan¹,
Anthony G. Pipe¹ and Tony J. Prescott²

¹*Bristol Robotics Laboratory, University of the West of England, Coldharbour Lane, Bristol BS16 1QD, UK*

²*Active Touch Laboratory, Department of Psychology, University of Sheffield, Sheffield S10 2TN, UK*

Active vibrissal touch can be used to replace or to supplement sensory systems such as computer vision and, therefore, improve the sensory capacity of mobile robots. This paper describes how arrays of whisker-like touch sensors have been incorporated onto mobile robot platforms taking inspiration from biology for their morphology and control. There were two motivations for this work: first, to build a physical platform on which to model, and therefore test, recent neuroethological hypotheses about vibrissal touch; second, to exploit the control strategies and morphology observed in the biological analogue to maximize the quality and quantity of tactile sensory information derived from the artificial whisker array. We describe the design of a new whiskered robot, *Shrewbot*, endowed with a biomimetic array of individually controlled whiskers and a neuroethologically inspired whisking pattern generation mechanism. We then present results showing how the morphology of the whisker array shapes the sensory surface surrounding the robot's head, and demonstrate the impact of active touch control on the sensory information that can be acquired by the robot. We show that adopting bio-inspired, low latency motor control of the rhythmic motion of the whiskers in response to contact-induced stimuli usefully constrains the sensory range, while also maximizing the number of whisker contacts. The robot experiments also demonstrate that the sensory consequences of active touch control can be usefully investigated in biomimetic robots.

Keywords: vibrissa; whisker; active touch; robot; biomimetic; whisking pattern generator

1. INTRODUCTION

Active touch, which implies a close coupling between motor and sensory systems, is an important biological observation that is of particular significance to robot engineering. The concept of feedback loops applied to sensorimotor systems is not new in robotics; however, the rapid tactile discriminatory ability of animals suggests that robotics could benefit from a close evaluation of the active touch sensing techniques employed in nature.

Tactile sensing systems based on thin, moveable, flexible shafts are a common feature of both invertebrates and vertebrates (see other articles in this issue). In mammals, such systems have evolved to exploit specialized exquisitely sensitive tactile hairs, or vibrissae, that reach their greatest levels of sophistication in rodents, such as rats and mice [1,2], and in pinnipeds and other aquatic mammals [3,4]. The long facial whiskers, or macrovibrissae, of rodents are particularly interesting when considered as active sensing devices, since controlled movement of the vibrissal shaft is a characteristic feature of this system. The

whiskers of many rodents, and also of some shrews and marsupials, are moved backwards and forwards during exploration of the environment, at rates of 7–10 Hz or more, in a behaviour known as ‘whisking’ [5–8]. Furthermore, the specific nature of the control exerted on the whisker shaft, during whisking, appears to be important for success in a number of sensory discrimination tasks [9–12].

The investigation of biomimetic artificial tactile sensing systems based on rodent vibrissae can serve two goals. First, a suitably designed and configured biomimetic robot platform could be useful for testing theories about natural vibrissal sensing systems. In particular, theories of active sensing posit that control of sensor movement acts to boost the task-related information that can be obtained from the sensory apparatus. Such hypotheses can be effectively explored in physical (robotic) models, perhaps more easily than in the biological systems they are designed to emulate [13,14]. Second, it can provide a useful engineering solution to the problem of sensing and navigation in robotics. Rodents use their vibrissae to explore and locomote on difficult terrain in the absence of light. A similar sensory capacity in mobile robots could lead to increased versatility and performance in hazardous environments, such as smoke- or dust-filled buildings, or where covert operation in darkness is required. Borrowing inspiration from marine mammals, similar systems might also find applications in

* Author for correspondence (martin.pearson@brl.ac.uk).

Electronic supplementary material is available at <http://dx.doi.org/10.1098/rstb.2011.0164> or via <http://rstb.royalsocietypublishing.org>.

One contribution of 18 to a Theo Murphy Meeting Issue ‘Active touch sensing’.

aquatic environments particularly in turbid water. Sensor tasks that are concerned with detecting material properties, such as measurement of texture or compliance, might also benefit from the use of vibrissal sensors that, in nature, approach the resolution of the human fingertip [15].

In this paper, we briefly summarize past research aimed at emulating the functional capacity of whisking animals in robots while also copying key aspects of animal morphology and sensory processing. We then present the latest in a series of whiskered robots that have been built through an iterative process of platform development and in which different aspects of active touch control have been explored. This new platform is inspired by the behavioural capabilities of the Etruscan shrew, which is able to detect and track moving prey in darkness (see [8]), hence its name *Shrewbot*. However, given the limited data available for that animal, and the generality of active touch sensing in whiskered animals [7], the design of *Shrewbot* is more broadly modelled on data from other animals including rats and mice. In this paper, we describe and assess the anatomically inspired whisker array morphology of the *Shrewbot* platform as well as the neuroethologically inspired whisking pattern generation (WPG) mechanism it uses. We then present results showing the impact of active touch control on the sensory information that can be acquired by the robot. We show that control strategies similar to those seen in whiskered mammals positively contribute to the quantity and quality of tactile signals available to *Shrewbot* and that the sensory consequences of modifying active touch control can be measured experimentally in biomimetic robots.

(a) *A brief history of biomimetic vibrissal touch*

Our work builds on a large number of previous research efforts in robotic tactile sensing systems recently reviewed in Prescott *et al.* [16]. Many of these past efforts were inspired by the impressive tactile discrimination abilities of whiskered animals and sought to investigate whether similar capabilities might be useful for autonomous machines. Research in this area began in the 1980s with Russell [17] who described a single stiff wire whisker whose position could be controlled in two dimensions. The sensor operated in both a scanning mode and an edge-tracing mode and was able to locate and follow the outline of detected objects. Russell specifically cited the cat vibrissal system as the inspiration for this system. While various forms of engineering-based or insect-inspired whisker-like sensing have been researched over the past 25 years, interest in more closely emulating active mammalian vibrissal sensing has flourished primarily in the last decade. Fend [18] developed an active whisking array consisting of real rat whiskers glued to condenser microphones. Bilateral rows of four whiskers were constructed and mounted on a small mobile robot (*Khepera*). All whiskers were moved together in a whisking-like motion at 0.7 Hz and through an arc of 40°. The authors demonstrated that the signals obtained from the whiskers during contacts with surfaces could be used for texture discrimination. Solomon & Hartmann [19]

used a single array of four steel whiskers, instrumented with strain gauges to measure whisker bending in two dimensions. The array was mounted on a pole, and swept against a small sculpted head using a single servo motor. They showed that the bending moment at the base of the whisker could be used to calculate the radial distance from the whisker base to the point of contact with the object and used this information to iteratively map out the three-dimensional shape of the sculpture. Kim & Moller [20] mounted two arrays of steel whiskers on actuated metal plates attached to a larger mobile robot (*Koala*). Both plates were rotated through a whisking arc of 50°, unless interrupted by an object contact, in which case they were programmed to move through an additional maximum of 21° of arc. Bending at the base of each whisker shaft was measured with a magnetic Hall effect sensor. The robot was able to distinguish a variety of geometrical shapes by using deflection angle and velocity from contacting whiskers.

While all of the above studies were strongly inspired by the vibrissal system of small mammals, and all used actuated vibrissae, their primary emphasis was on the extraction of object properties from whisker-surface contacts rather than on the control of the whiskers, and on the impact of this control on sensing, *per se*. In contrast, our own research has directly focused on emulating, in a more detailed manner, the types of active sensing control observed in animal vibrissal movements, with the specific aim of improving the quality and/or quantity of sensory information obtained. To introduce this research, we first briefly review a number of the design issues, and relevant experimental findings from studies of natural vibrissal touch, and summarize how these have inspired and motivated this work.

(b) *Morphology and control of the vibrissal array*

The morphology of the whisker array of an animal describes the distribution of the whiskers on the head, the length and the structure of the whisker shafts, and the degrees of freedom in the movement of both the whiskers and the mystacial pad into which they are anchored [21,22]. The morphological properties of the rat vibrissal system have been analysed in detail by Towal *et al.* [22], Hartmann and co-workers [23] and Birdwell *et al.* [24] who have shown that they make a significant contribution to the types of signals obtained through whisker-environment contacts. Here, we briefly discuss morphological features of biological vibrissal systems and their artificial counterparts together with sensor transduction and aspects of active sensing control.

Many mammals possess arrays of macrovibrissae that emerge from muscular, collagen-dense mystacial pads located above the upper lip [25,26]. Although a roughly grid-like arrangement of whiskers in each pad is a typical feature, the number of whiskers in each row and column varies with species. Rats and shrews have up to 30–40 macrovibrissae per side, most species also have significant numbers of shorter and non-actuated microvibrissae on the lips and chin. In adult rats, the longest whiskers reach around 50 mm in length while in the tiny Etruscan shrew they are around 12 mm. In both species, the span of

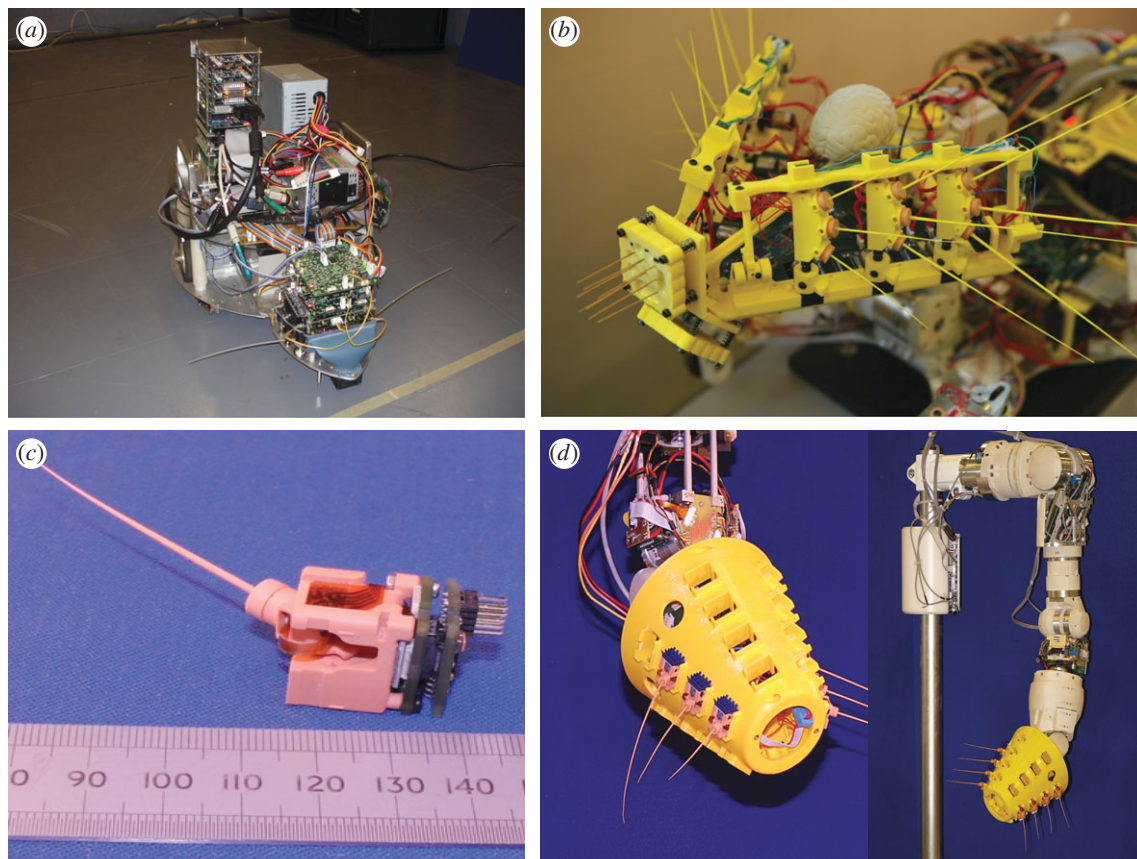


Figure 1. Photographs of whiskered robots developed by the authors. (a) Whiskerbot was completed in 2005, in the configuration shown it had two active whiskers formed from glass-fibre and used a detailed spiking neural model of the follicle sinus complex to transduce whisker deflection signals into model spike trains. (b) SCRATCHbot was built in 2008, incorporating a 3 d.f. neck and an array of 18 active plastic whiskers with separate per-column control, the platform was used to investigate biomimetic models of sensory noise cancellation and three-dimensional orienting. (c) In 2009, the BIOTACT whisker module was developed to provide a compact, independent whisker sensor with integrated motor, controller and sensory processing. (d) The BIOTACT sensor, constructed in 2010, demonstrates how individual whisker modules can be combined into arrays, in this case mounted as the end-effector of a 7 d.f. robotic manipulator.

the whisker array considerably exceeds the width of the animal. Another cross-species characteristic of whiskered land mammals is an exponential distribution in the length of the macrovibrissae protruding from the mystacial pad along each row of the array, i.e. the more rostral macrovibrissae are exponentially shorter than the more caudal whiskers in the same row. In contrast, measures of the distribution in lengths of macrovibrissae across the array have found no strong dorsal-ventral trend [21,22].

We can consider the tips of macrovibrissae as defining a two-dimensional *sensory surface* that surrounds the head when the whiskers are at rest, and that moves through space as the whiskers are actuated. Intuitively, a larger more flexible sensory surface will assist the animal/robot to infer macrogeometric properties of surfaces by being able to physically replicate the surface form in the whisker field. Although the macrovibrissal array of mammals has significant asymmetry in the ventro-dorsal dimension, and is composed of two distinct vibrissal arrays, the sensory surface generated by the whisker tips during exploration has a surprising degree of radial symmetry. Indeed, when the whiskers are moved against a flat surface in front of the rat, the spread of whisker contacts forms a near radial pattern

described by Hartmann *et al.* [27] as resembling the ‘spokes of a wheel’.

Most whiskered robots have been configured with relatively few vibrissae, and research has often focused on the possibility of using single whiskers to detect microgeometric features such as surface texture. However, the large, fast-moving vibrissal arrays of rodents suggest that contact with a single whisker is a rare event in biology, and that the integration of information across the sensory array is likely to form an important component of natural vibrissal sensing. Robots have also hitherto been developed with little consideration for the geometry of the whisker system, we have therefore begun to specifically investigate these issues and report some initial results on the shape of the sensory surface generated by our whisking robots in §2 below.

The macrovibrissae of land mammals are usually tapered, smooth and curved [28]. With the exception of Fend [18], most previous whiskered robots have used steel wire whiskers that are under-damped compared with biological whiskers [23] and, therefore, prone to excessive oscillation during whisker motion. Since our aim is to make artificial vibrissae suitable for different-sized mobile robot platforms, we have experimented with a range of different light-weight

and flexible materials in our robot models. Our aim has been to qualitatively copy some of the important characteristics of whiskers without necessarily replicating all of their specific physical properties. For example, the tapering of whiskers has been demonstrated to have a substantial effect on models of static sensing [24] and on the robustness of their frequency response [28]. Rapid prototyping technology allows us to custom build our artificial whiskers to incorporate different rates of taper so as to exploit these observations and explore their possible advantages. The grid-based topology and whisker length distribution across the mystacial pad are further examples of established cross-species morphological features that we have qualitatively incorporated into our physical models, comparison between such morphologies being one of the key themes of this paper.

Mammalian whiskers are anchored in large and mechanically complex follicles that contain many hundreds of mechanoreceptors of different types [29,30]. Processing in these receptors and in the primary afferent neurons that they supply is known to be able to transduce small deflections of the vibrissal shaft with good fidelity and to encode information about velocity, amplitude and direction of whisker deflection [31]. In rats, the angular position of the whisker is also thought to be encoded by sensory nerves that innervate the whisker follicle and surrounding tissue [32]. These observations suggest the need to encode at least two dimensions of whisker motion in artificial vibrissal systems, and to be able to measure the instantaneous angular position of each whisker.

The rat vibrissal system has a sophisticated musculature consisting of a set of *extrinsic* muscles that move the whisker pad relative to the skull and *intrinsic* muscles connecting pairs of whiskers in a row-based scheme [33]. However, analyses of the kinematics of rat exploratory whisking show that the principle component of most whisker motion is a repeated and rapid anterior-posterior sweep (see [7, 34–36]). The forward protraction phase of whisking is brought about by a combination of activity in the intrinsic and extrinsic muscles and backward retraction by a mix of extrinsic muscle activity and skin elasticity [37]. Similar to earlier robot models with actuated vibrissae, we have chosen to focus on this principle degree of freedom of movement of the macrovibrissae in our platforms. However, in contrast to those models, we have opted to allow for some independent actuation of single whiskers or whisker columns. Although this considerably complicates the design of the whisker apparatus it has allowed the possibility of exploring a wide range of whisker movement patterns that can include modulation of the movement of groups of whiskers according to context. Specifically, recent research by our own group and others (see [7] for review) has shown, in several whisking mammal species, that the behavioural context, the movement of the animal, or contacts with objects, can all induce changes in the whisking patterns expressed by animals. We next briefly describe some of the modulations in exploratory whisking behaviour that appear to be induced by contacts with surfaces or objects of interest and that we have sought to reproduce in our robots.

A common form of contact-related modulation, observed in multiple species [7,38], is that whisker protraction is controlled following a unilateral contact, such that whiskers on the side of the snout ipsilateral to the contact are reined in and those on the contralateral side brought forward, sometimes contacting another part of the encountered obstruction and resulting in bilateral contact. We refer to this observation as *contact-induced asymmetry* (CIA, [7]). Contact with a surface of interest also often initiates a *rapid cessation of protraction* (RCP) of the contacting whiskers [7,36], while observation of post-contact whisking behaviour shows that the reduced protraction of contacting whiskers is typically accompanied by increased protraction of more caudal (non-contacting) whiskers, leading to an overall reduction in the angular separation, or *spread* of the whisker field [36]. Finally, under some conditions, it appears that contact leads to RCP, but also to a subsequent *reignition* of protraction (see figure 4). Thus, the whiskers may sometimes detach completely from the contacted surface and then contact it a second time within the course of the same whisk cycle, an observation we refer to as *double touch* ([39], figure 4). Note that biphasic protractions are also seen during whisking in air [40], where they are referred to as *double pumps*. The circumstances under which double pumps occur are discussed in Mitchinson *et al.* [7] and, since they do not appear to be contact-related, they are not considered further here.

Altogether, these observations (CIA, RCP and spread reduction) can be characterized as involving reduced protraction of whiskers that are close to a contacted object and increased protraction of whiskers that are further away. Whisking control is therefore consistent with our hypothesis of an overall strategy of *minimal impingement/maximal contact* (MIMC), whereby the animal seeks to make as many contacts as possible, but to make those contacts with a ‘light touch’ [7,38]. Maximal contact is clearly a strategy that tends to maximize information quantity. We have suggested that minimal impingement may be a useful strategy for maximizing information quality, since contact events will tend to be normalized (i.e. will cover a reduced dynamic range).

(c) *Biomimetic active vibrissal touch systems*

We have developed a number of biomimetic robot platforms designed to investigate the impact of the above characteristics of biological vibrissal systems on active touch sensing. We next briefly review the design features and experimental results from a number of our earlier platforms before describing our latest robot. For further detail of these earlier systems see [14,16,41–43].

Our first robot, *Whiskerbot* [41] (figure 1*a*), possessed a bilateral array of moulded glass fibre whiskers that were tapered and curved to resemble rat whiskers at approximately 4 × the scale (200 mm). Each whisker was equipped with strain gauges to measure bending in two dimensions. Whisker actuation used a material termed shape-memory alloy. Passing current through this material generates heat causing a linear muscle-like contraction which generated whisker protraction,

with springs causing the whiskers to retract to their starting position. This system was able to whisk at up to 5 Hz when fans were used to cool the actuating wires. Signals from whisker contacts were transduced through a model of the rat follicle and primary afferent nerve [30] to generate artificial spike trains similar to those recorded in the trigeminal ganglion of rats [32]. Experiments showed the ability of the robot to orient to targets detected using the vibrissae via systems-level models of appropriate rat brain systems [41]. Both negative and positive feedback loops were employed to modulate whisker actuation based on object contacts with tests providing proof-of-principle that these mechanisms can be used to constrain the dynamic range of contact signals and promote increased numbers of contacts.

Although Whiskerbot was designed to carry multiple whiskers per side, the constraints of using shape memory alloy actuation made it difficult to mount and control multiple independently actuated macrovibrissae on each side of the snout. A further problem was the lack of degrees-of-freedom (d.f.) for positioning the robot head, which was rigidly fixed to the robot body. This essentially limited Whiskerbot to exploring vertical surfaces near ground level. Meanwhile, our research with rats increasingly demonstrated the importance of movements of the head and neck in positioning the vibrissal array in whiskered animals [36]. To overcome these limitations, and others, we therefore developed a completely new whiskered robot platform, *SCRATCHbot* [14,42] (figure 1*b*). Three whisker carriers were mounted on either side of *SCRATCHbot*'s light-weight plastic head, with each carrier holding three whiskers in a vertical column. The geometry of the head was such that all the whiskers would point directly ahead of the robot when fully protracted with each column able to rotate through 120°. A second dorsoventral actuated axis of rotation was also implemented, limited to a single actuator for each side (rotating all three columns simultaneously), and constrained to $\pm 15^\circ$ of rotation about the vertical. This degree of freedom allowed the whiskers to be oriented towards surfaces of interest at different vertical heights compensating somewhat for the small number of whiskers in each array compared with a whiskered mammal. To overcome the problems of actuation using shape memory alloy, whisker movement used standard DC motors equipped with shaft encoders to allow accurate measurement of the whisker angular position. We also switched to using tri-axis magnetic Hall effect sensors (similar to Kim & Möller [20]) to transduce whisker deflection signals owing to reliability issues with the strain gauges used with Whiskerbot. A small magnet, attached to the base of the whisker shaft, moves relative to an electric field within the Hall effect sensor allowing lateral movement to be measured along two axes (x and y) and axial movement (parallel with the whisker shaft) along a third (z). Tapered, flexible plastic vibrissal shafts were constructed using a rapid prototyping machine. Whisker-guided orienting, using a model of the mammalian superior colliculus was extended in *SCRATCHbot* to three dimensions [42], and we developed a model of sensory noise cancellation [44], inspired by the mammalian cerebellum, to overcome the problem of false-

positive whisker deflection signals generated by the robot's own movement. Feedback control of vibrissal movement was extended to replicate experimental findings with rats including the reduction of whisker spread following contact [14,36].

The next evolution of active vibrissal touch systems was to develop a completely modular artificial whisker, incorporating its own actuation mechanism and control electronics, that could be assembled into different sensor configurations. The *BIOTACT whisker module* (see [43] and figure 1*c*) makes use of a miniature brushless DC motor with closed-loop *proportional derivative* (PD) control provided by an on-board microcontroller. The modules are $20 \times 15 \times 15$ mm in size and capable of whisking through a 90° arc at frequencies of up to 10 Hz. Deflection of the whisker shaft is again detected using an embedded Hall effect sensor. Modular whiskers have been assembled onto a sensory cone, termed the *BIOTACT Sensor*, that has been mounted on a robot arm (shown in figure 1*d*) and used for experiments in artificial texture discrimination and radial distance detection for which a number of novel classifier tactile pattern recognition systems have been developed [43].

2. SHREWBOT: A PLATFORM FOR INVESTIGATING BIOMIMETIC MORPHOLOGY AND CONTROL IN VIBRISSAL ACTIVE TOUCH

The development of our modular artificial whisker presented the opportunity to rethink the design of our whiskered mobile robots, which led to the development of our latest platform, *Shrewbot*, which is illustrated in figure 2 together with a diagram of its embedded processing and control architecture. The robot consists of a commercially available wheeled robot base called a *Robotino* [45] augmented with additional computing resources and a 3 d.f. neck, similar to that used on *SCRATCHbot*. The head is mounted as the end-effector on the neck and is populated with 18 individually actuated macrovibrissae and electronics similar to the *BIOTACT Sensor*. We also plan to add a central microvibrissal array of 12 short, non-actuated whiskers to the tip of the snout. The *Robotino* is not biomimetic, rather it was chosen for its robustness and manoeuvrability through the non-holomically constrained omni-drive. As in *SCRATCHbot*, the neck and head are designed to qualitatively emulate the main degrees of freedom of the head-positioning system of a small mammal. The main innovation from a biomimetic point of view is, therefore, in the morphology of the snout and its macrovibrissal array.

Shrewbot has six rows of three columns of whiskers, which, unlike *SCRATCHbot*, are distributed radially around the robot head mounted onto discs distributed along a central column. This design, therefore, accentuates the radial symmetry of the vibrissal array, which was noted above to be a characteristic of the sensory surface afforded by the macrovibrissae of rats. In keeping with this radial design, different lengths of whisker were built to occupy the different columns of each row, with the different rows identical. The most rostral column is populated with 60 mm long whiskers, the middle column 98 mm and the most caudal 160 mm. Thus, *Shrewbot*'s array is around $3.2 \times$ the scale of the

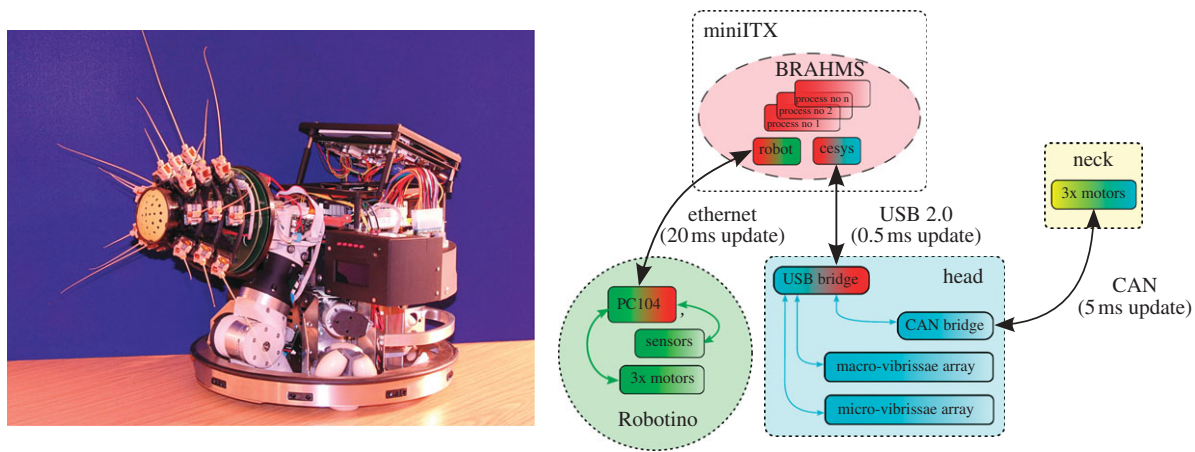


Figure 2. Photograph of Shrewbot with a block diagram of its main physical components and their inter-connectivity and update rates. Shrewbot consists of a Robotino platform augmented with a miniITX computer, a 3 d.f. neck and a head composed of 18 individually actuated macrovibrissae. Each whisker module consists of a motor and shaft encoder, a 3-axis Hall effect sensor, and an embedded microprocessor. See main text for a full description of the robot and the electronic supplementary material for a more detailed account of the robot control architecture.

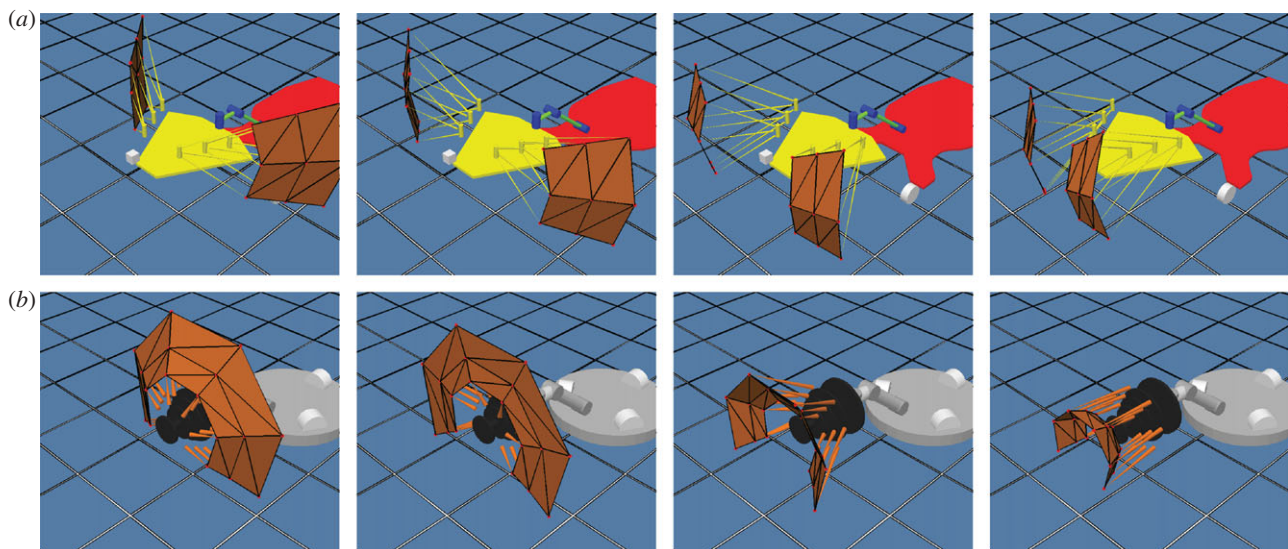


Figure 3. Still frames taken from a simulated rendering of (a) SCRATCHbot and (b) Shrewbot emphasizing the form of their whisker fields and inferred sensory surface, interpolated between the whisker tips (shown in brown), at different phases of whisking. Shrewbot is able to form a radially symmetric sensory surface with a concave or convex profile similar to that observed in rats [27,22]. The less biomimetic whisker array morphology of SCRATCHbot is incapable of forming a convex sensory surface.

rat and $13 \times$ the scale of the shrew if judged by the metric of whisker length. Following our earlier experiments with a range of materials for whisker shafts we selected *NanoCure RC25*, a nanoparticle-filled material that generates a strong, temperature-resistant composite, as providing a good compromise between flexibility, robustness to breakage and ease of manufacture. Using a rapid prototyping machine, we were able to construct whiskers of different lengths with a tapered profile and reasonably smooth exterior. Although not manufactured to have specific curvature, the whiskers sometimes also cured to have a mildly curved profile.

Figure 3 illustrates the sensory surface of Shrewbot compared with our earlier whiskered robot SCRATCHbot, generated using an accurate computational model of the vibrissal geometry and kinematic constraints of both platforms. The processing architecture of each

robot (described further in the electronic supplementary material) can drive either this simulated model of the platform or the physical robot itself, to facilitate platform development. Similarly, either the simulated odometry from the computational model or the real odometry from a live robot experiment can then be graphically replayed using MATLAB. From this graphical rendering of such a simulation, it is clear that the sensory surface of Shrewbot has potential advantages over SCRATCHbot for spatial exploration. Specifically, the surface surrounds the head in a continuous fashion and can be formed into both concave and convex shapes as has been described for rats [22]. The ability to form a smooth convex surface (with respect to the robot), when the whiskers are fully protracted, is largely owing to the exponential increase in length of the whiskers along the row. A linear increase in whisker length

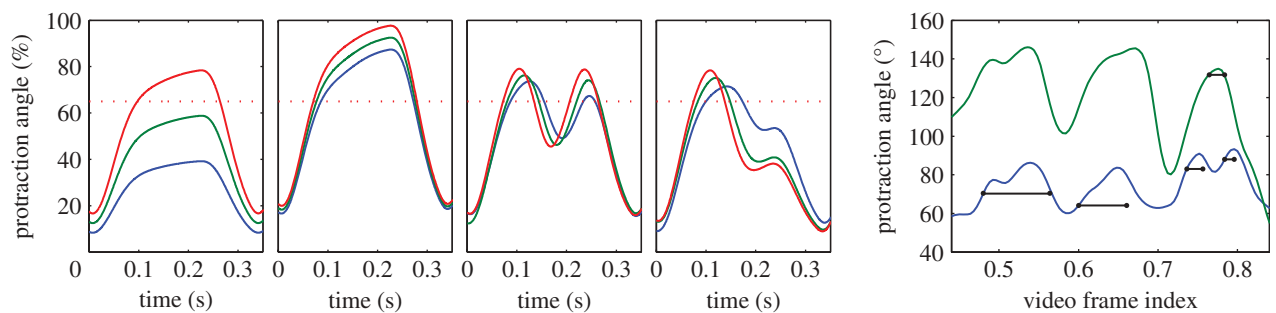


Figure 4. Each of the four panels on the left show the time progression of the protraction angles of a Shrewbot whisker from each of the caudal (blue), central (green) and rostral (red) columns during a simulated movement against an obstruction at 60% protraction (dotted red line). Panels display results for different contact-induced modulation strategies. From left to right: *WPG1*—with no modulation, only the rostral whisker contacts. *WPG2*—contact-induced modulation causes all whiskers to be excited forward and make contact, owing to excitation from contact in the previous whisk; in the case of a genuine contact, this would result in considerable bending of the more rostral whiskers. *WPG3*—‘feedback’ inhibition reduces the impingement of all whiskers, but leads to double-touch. *WPG4*—‘release’ includes a heuristic for suppressing double-touch. Far right panel shows approximately 400 ms of results from manual tracking of real rat whiskers during interaction with an object. Each trace shows the mean whisker angle on the left (blue) and right (green) of the snout; black lines indicate the time windows within which the whiskers on that side were in contact with the environment. Three whiskers are shown. All three whiskers show evidence of CIA—protraction is much reduced on the left side compared with the right. The final whisker shows an episode of ‘double-touch’ on the left-hand side (i.e. two separate regions of touch occur within the same whisk cycle).

along the row would result in a more ‘conical’ surface form when fully protracted. The implication of either configuration has yet to be fully evaluated, however, biological data from the rat does appear to suggest advantages for the convex form [22] and it would be interesting to see if this result is replicated in other whiskered animal species.

(a) *Shrewbot’s active touch control*

The contact-induced modulations observed in animals were summarized above as resulting in reduced protraction in contacting whiskers and increased protraction of non-contacting whiskers. The hypothesis of MIMC suggests that an optimal control system might control each whisker independently, for instance, by combining local (single whisker) inhibition alongside global excitation. The data to reveal whether the animal can exert this level of control are currently lacking, however, and it is possible that the animal approximates this with control over groups of whiskers or in a way that is better described as control of the sensory surface (figure 3) with less degrees of freedom than there are whiskers. The individual whisker control afforded by the design of Shrewbot allows us to investigate a range of options, a number of which are explored below. Here we describe, in general and qualitative terms, the operation of the underlying WPG used in Shrewbot and four variants we have tested on the robot. A full mathematical description of these algorithms is provided in the electronic supplementary material.

In the absence of object contacts, and continuously in the case of the unmodulated *WPG1*, whiskers in each column (caudal, central, rostral) are protracted towards approximately 40, 60 and 80 per cent, respectively, of maximum protraction, approximating the caudal-to-rostral pattern of whisker spread during protraction seen in the animal [36], with all whiskers moving towards 0 per cent (maximum retraction) in

the retraction part of each cycle. All whiskers are driven by a single global clock, protracting/retracting for 70/30 per cent of each ‘whisk period’ (0.333 s), and their instantaneous angle is a first-order response to the clock signal. The leftmost panel of figure 4 shows the trajectory of whiskers, for an example, whisk for the unmodulated WPG.

Next, we derive a signal called *contact belief* from the raw displacement signals returned from the Hall effect sensors at the bases of the whiskers. In recent work [44], we have developed a cerebellum-inspired model for the optimal removal of noise in these raw signals owing to self-movement (of the whiskers, and of the head); here, we use a simple threshold-and-saturate function to eliminate spurious self-generated signals and return a single value for contact belief from the combined x/y displacement of each individual whisker. This signal, denoted $c_w \in [0,1]$ for the w th whisker, is the sole source of pattern modulation for all of the modulated WPGs.

Each of the three modulated WPGs implements some version of global excitation of the whisker field following contact, with or without some variant of local inhibition of contacted whiskers. Global excitation is implemented by taking the maximum of c_w across all whiskers, and using this to raise the maximum protraction of all whiskers towards 100 per cent (strong contact belief, thus, leads to all whiskers protracting strongly forwards). This excitatory influence, and subsequent increase in protraction angle, decays with a time constant of 1 s in the absence of further whisker contacts (see equation 2 in the electronic supplementary material). Local inhibition is implemented in two forms, denoted ‘feedback’ and ‘release’. In ‘feedback’, the instantaneous value of c_w inhibits protraction of the w th whisker. With appropriate geometry (which often occurs), inhibition leads to detachment of the whisker from a surface, cessation of the inhibition signal, reignition of protraction and double-touch. Thus, this demonstrates a plausible

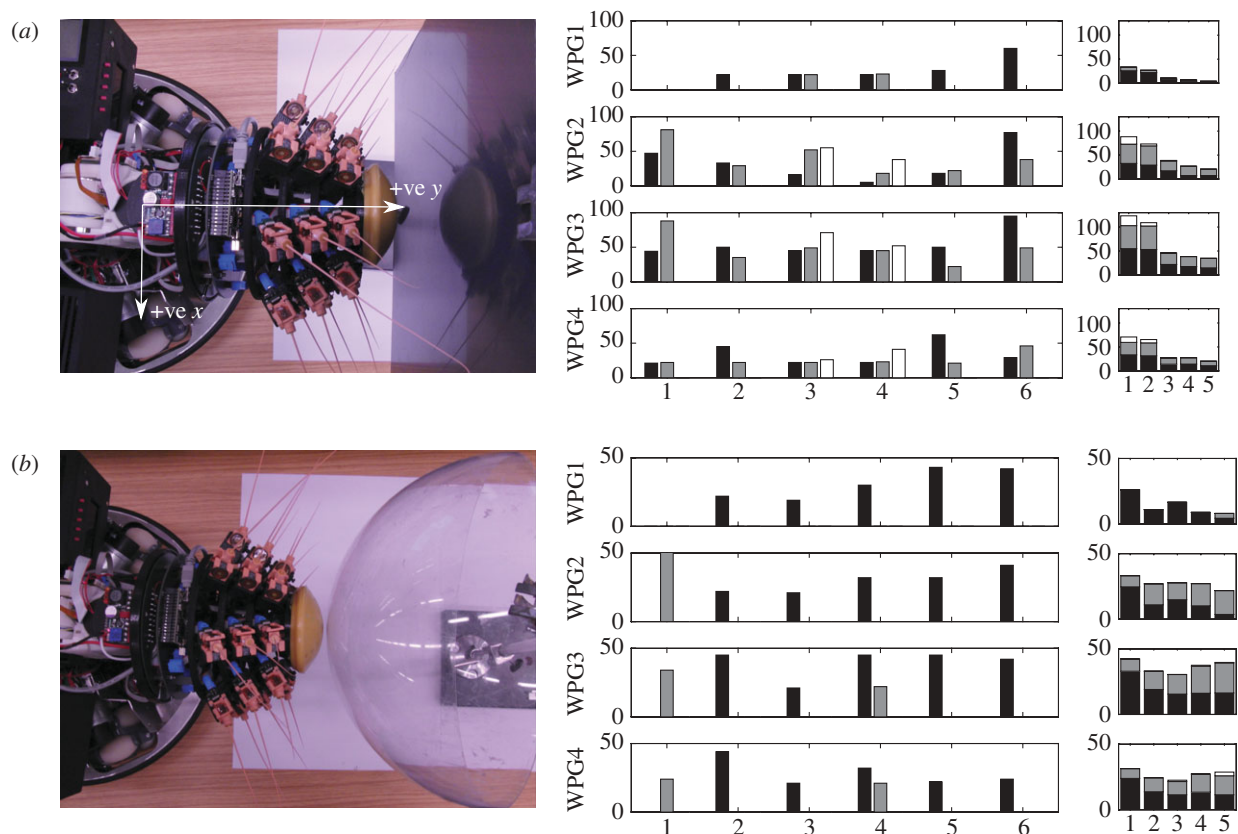


Figure 5. (a,b) Photographs of the experimental set-up and bar plots representing the number of contacts made by all 18 whiskers during a 10 s bout of 3 Hz whisking against two different surfaces—(a) FLAT and (b) CONVEX—at five different horizontal positions and using the four WPG configurations: *WPG1*—without feedback, *WPG2*—with global excitation alone; *WPG3*—with both global excitatory and local inhibitory feedback and *WPG4*—with global excitation and using the ‘release’ model of local inhibition. The central panels show the total number of contacts per whisker using each of the four WPG configurations for the case where the surface is in the central position (referred to in the text as position 1). Here, the bars are arranged into groups by radially separated row, the shade of each bar in a group indicating which column the whisker was in—black, most rostral; grey, middle; and white, most caudal. The right panels present the average number of contacts for all rows (columns stacked) using each WPG configuration and at each of the five positions of the surface along the head-centric x -axis of the robot.

mechanism for the observation of double-touch in the animal, as an oscillation in a negative feedback loop with significant time lag. In ‘release’, the same instantaneous inhibition is used as for ‘feedback’, but an additional mechanism is used to suppress double-touch events. Thus release implements a simple form of minimal impingement (no double-touch events). Three specific-modulated configurations are used in the experimental section, for which example trajectories are illustrated in figure 4, these are: *WPG2* (global excitation alone), *WPG3* (global excitation and ‘feedback’ local inhibition) and *WPG4* (global excitation and ‘release’ local inhibition).

3. EXPERIMENTAL EVALUATION OF ACTIVE TOUCH CONTROL STRATEGIES

As noted in §1*b* above, analyses of high-speed video recordings of whisking animals have suggested the hypothesis that modulation of whisker movement patterns using contact-related feedback can increase the number of contacts made with surfaces of interest, while constraining the dynamic range of the signals obtained (leading to greater fidelity of representation of signals within that range). Experiments with our

earlier whiskered robot platforms have supported the claim that feedback control can improve discrimination performance, but we have not previously analysed the effects of feedback on signal metrics. In this section, we report a simple experiment to address this, in which Shrewbot explores two surfaces with different geometry using the four alternative WPG models described above. A short movie showing Shrewbot’s exploratory behaviour, using both head, body and whisker movements (controlled by *WPG4*) is provided in the electronic supplementary material.

(a) Methods

The Shrewbot platform was placed on a bench with the neck and wheel motors immobilized. A clamp stand was positioned in front of the whisker field, such that two surfaces, hereafter referred to as *FLAT* and *CONVEX*, could be suspended close to the tip of the snout (see photographs in figure 5). *FLAT* was a square sheet of smooth Perspex, side length of 300 mm; *CONVEX* was a Perspex hemisphere, 150 mm radius. Both surfaces were aligned parallel to the head-centric x - and z -axes and perpendicular to the y -axis (see figure 5 for reference), with the centre of mass of each surface

initially set at (x,y,z) position (0, 210 mm, 0). Ten second bouts of 3 Hz whisking were then recorded against each surface using the four different configurations of the WPG described in §2a. Each surface was then translated along the head-centric x -axis to five set locations and the 10 s bouts of whisking using each WPG configuration repeated. For FLAT, these locations were: 0 (position 1), +60 (position 2), +120 (position 3), +180 (position 4) and +220 mm (position 5); for CONVEX they were: 0, +20, +40, +60 and +80 mm.

These data were processed to determine the number and nature of contacts that were made by the whiskers during each 10 s bout. Each contiguous region of non-zero values in the contact belief signal was defined as a ‘contact event’. For each contact event, three metrics of contact magnitude were obtained. First, ‘contact depth’ was defined as the mean absolute value during the event of the raw deflection signal in the x -dimension (rostral to caudal). Second, ‘contact duration’ was defined as the duration of the event in sample periods. Third, ‘contact impulse’ was defined as the product of the previous two metrics (equivalently, as the integral of the absolute value of the x signal across the event).

(b) Results

For both surface types, and for all different surface positions, the use of WPG2 leads, as expected, to an increase in the number of contact events when compared with WPG1. Results are broken down by row and column in figure 5 and summarized across all whiskers in figure 6. WPG3, despite introducing inhibition, actually increases the number of contact events further, owing to the conversion of single-touch whiskers into double-touch whiskers. WPG4, also as expected, reduces the number of contacts in all cases with respect to results for WPG3, in most cases to slightly less than the number generated by WPG2, as many double-touch whiskers are eliminated. Overall, across both surfaces and all positions, WPGs 2, 3 and 4 generated 2.6, 3.5 and 2.3 times as many contacts, respectively, as unmodulated whisking (WPG1). Figure 6 presents the ratio of the total number of contacts for modulated WPG configuration (2, 3 and 4) against un-modulated (WPG1) for each surface and at each position. This analysis shows that the increase in the number of whisker contacts, for modulated WPGs, is particularly evident when the surface is located further from the centre of the array. Correspondingly, the strategy of excitatory whisker control may be particularly advantageous in configurations where the head is not optimally positioned to explore the surface being investigated (e.g. if the contacted object is not at front and centre with respect to the animal).

If the quantity of whisker contacts were the only performance criterion then, in the context of this simple experiment, the WPG3 ‘feedback’ model would be the optimal choice among the tested WPG models. However, the quality of the contacts generated must also be a criterion. One possible metric of contact quality is dynamic range—if the dynamic range is controlled, information loss owing to small contacts falling below the noise floor or owing to large contacts overloading the sensors can be avoided. Thus, in figure 7, we analyse

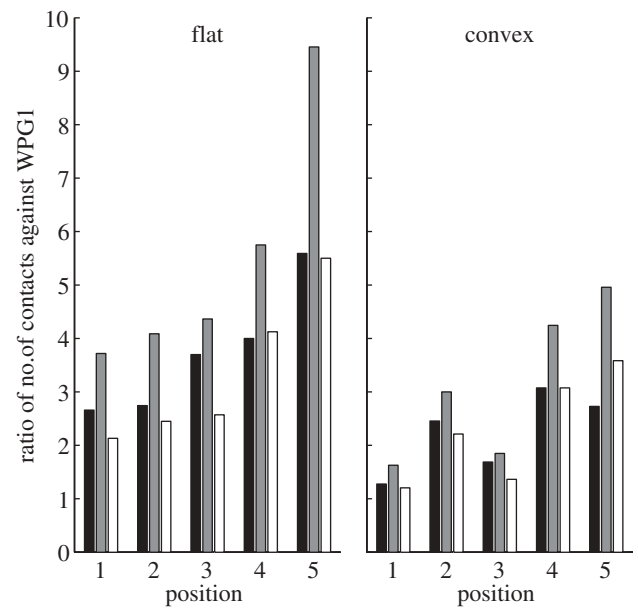


Figure 6. Ratio of the total number of contacts by all whiskers in the array using different WPG configurations compared with the number recorded using WPG1 at the five different positions for each surface. Black bars, WPG2; grey bars, WPG3; white bars, WPG4.

the three metrics of contact magnitude, defined above: contact depth, duration and impulse. Examining the leftmost column of histograms, we can see that the variability of contact depth is lowest in the pattern generation models that include inhibition (WPG3 and WPG4). Even more marked is the tightening of the distribution of contact duration using inhibitory control (middle column). Consequently, the variability in contact impulse (defined as the integral of contact depth over the period of the contact) is greatly reduced, primarily in this condition owing to a reduced variability in contact duration. In summary, the reduced variability in all of these measures, when control involves some form of minimal impingement, indicates a narrowing of the dynamic range of the contact signals.

4. DISCUSSION

Consideration of the morphology and sensorimotor coordination of facial whisker arrays in animals has guided the design, and improved the performance, of a robot with a vibrissa-like sensory array. Building biomimetic arrays of artificial whiskers has also provided us with the opportunity to develop and test hypotheses about the active touch control strategies employed by animals through physical implementation. In particular, we have shown above that the contact-driven feedback control of whisking, apparent in the behaviour of rats and other small mammals [7], may increase both the quantity and the quality of vibrissal sensory information. Our next steps will be to investigate the specific impacts of these forms of control on performance in sensory tasks that whiskered mammals are known to be good at, and to establish whether there are *task-specific* modulations of whisker movement that are effective in both animals and robots. An important question that we are currently investigating through

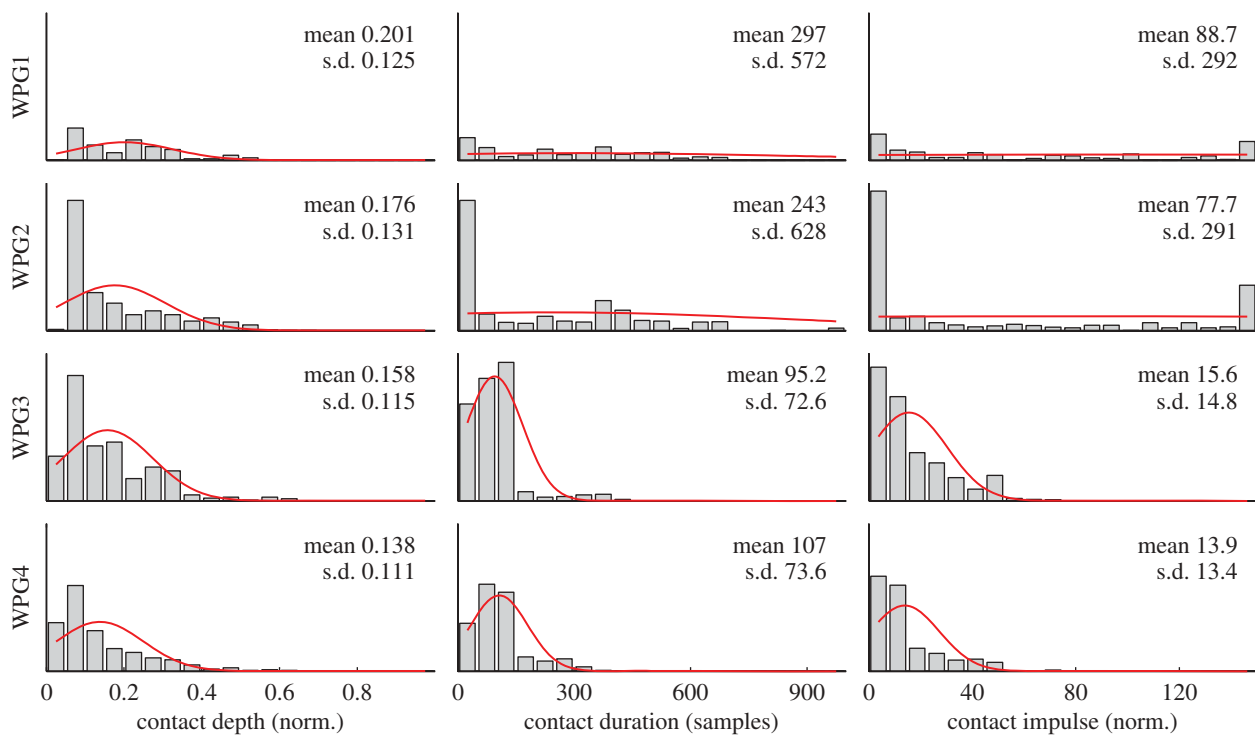


Figure 7. Distributions of magnitudes of contact depth, duration and impulse for all whisker contact events recorded using the four WPG configurations across all positions against both surfaces. *Contact depth* is the mean of the absolute value of the sensor x -displacement during a contact event, normalized to maximum sensor displacement; *Contact duration* is the length of time in 500 μ s samples of a contact event; *Contact impulse* is the area under the absolute x -displacement during a contact event. Normal fit for each distribution overlaid in red, with the frequency of each measure represented in the y -axis of each plot (0–700).

behavioural studies is whether active touch control is experience-dependent, that is, do animals adapt their patterns of whisking motor control to improve sensory performance either during development, or while learning a task? Preliminary evidence suggests a positive answer to both of these questions [12,46].

A key finding of our ethological and robotic studies is that minimal impingement, or ‘lightness of touch’, shown here as resulting in reduced dynamic range, is an important component of sensor control. We are currently conducting further investigations of the impact of control of dynamic range on pattern recognition algorithms for artificial whiskers [47,48], in order to show, quantitatively, how this affects performance. It is known that people also carefully regulate the pressure of fingertip touch during haptic tasks [49,50], in other words, minimal impingement may well be a generic strategy for active touch regardless of whether the interface to the world is a sensitive pad of skin or a flexible whisker.

The neural substrate for WPG in rodents has yet to be fully understood, although it is known to involve a complex architecture composed of multiple sensorimotor loops [51], potentially with dissociable circuits that regulate different control parameters [52]. The development of a physical model of the vibrissal system allows us to embed and test computational neuroscience models of the brain circuits involved in vibrissal sensory processing and control [41]. In the future, we therefore expect to be able to develop and test increasingly rich models of the neural and physical substrates of complex touch-guided behaviours such as shrew predation [8] using our biomimetic whiskered robots.

This research was funded by the European Union Future Emerging Technologies Programme via the BIOTACT project (ICT-215910). The authors are grateful for the support and advice of members of the Bristol Robotics Laboratory (BRL) and of the Active Touch Laboratory in Sheffield. We would also like to acknowledge the intellectual ideas and encouragement of members of the BIOTACT project, in particular, the laboratory of Michael Brecht in Berlin, whose work on the Etruscan Shrew provided some of the inspiration for the development of Shrewbot. We would also like to thank Robyn Grant, Charles Fox, Ehud Ahissar, and Mitra Hartmann for helping to develop ideas about active sensing control in animals and robots.

REFERENCES

- Vincent, S. B. 1912 The function of vibrissae in the behaviour of the white rat. *Behav. Monogr.* **1**, 1–81.
- Welker, W. I. 1964 Analysis of sniffing of the albino rat. *Behaviour* **22**, 223–244. (doi:10.1163/156853964X00030)
- Zimmer, C. 2011 By a whisker, harbor seals catch their prey. *Science* **293**, 29–31. (doi:10.1126/science.293.5527.29b)
- Dehnhardt, G., Mauck, B., Hanke, W. & Bleckmann, H. 2001 Hydrodynamic trail-following in harbor seals (*Phoca vitulina*). *Science* **293**, 102–104. (doi:10.1126/science.1060514)
- Zucker, E. & Welker, W. I. 1969 Coding of somatic sensory input by vibrissae neurons in the rat's trigeminal ganglion. *Brain Res.* **12**, 138–156. (doi:10.1016/0006-8993(69)90061-4)
- Wineski, L. E. 1983 Movements of the cranial vibrissae in the golden-hamster (*Mesocricetus auratus*). *J. Zool.* **200**, 261–280. (doi:10.1111/j.1469-7998.1983.tb05788.x)

- 7 Mitchinson, B., Grant, R. A., Arkley, K., Rankov, V., Perkon, I. & Prescott, T. J. 2011 Active vibrissal sensing in rodents and marsupials. *Phil. Trans. R. Soc. B* **366**, 3037–3048. (doi:10.1098/rstb.2011.0156)
- 8 Brecht, M., Naumann, R., Anjum, F., Wolfe, J., Munz, M., Mende, C. & Roth-Alpermann, C. 2011 The neurobiology of Etruscan shrew active touch. *Phil. Trans. R. Soc. B* **366**, 3026–3036. (doi:10.1098/rstb.2011.0160)
- 9 Carvell, G. E. & Simons, D. J. 1995 Task- and subject-related differences in sensorimotor behavior during active touch. *Somatosens. Mot. Res.* **12**, 1–9. (doi:10.3109/08990229509063138)
- 10 Knutsen, P. M., Pietr, M. & Ahissar, E. 2006 Haptic object localization in the vibrissal system: behavior and performance. *J. Neurosci.* **26**, 8451–8464. (doi:10.1523/JNEUROSCI.1516-06.2006)
- 11 O'Connor, D. H., Clack, N. G., Huber, D., Komiyama, T., Myers, E. W. & Svoboda, K. 2010 Vibrissa-based object localization in head-fixed mice. *J. Neurosci.* **30**, 1947–1967. (doi:10.1523/JNEUROSCI.3762-09.2010)
- 12 Zuo, Y., Perkon, I. & Diamond, M. E. 2011 Whisking and whisker kinematics during a texture classification task. *Phil. Trans. R. Soc. B* **366**, 3058–3069. (doi:10.1098/rstb.2011.0161)
- 13 Webb, B. 2001 Can robots make good models of biological behaviour? *Behav. Brain Sci.* **24**, 1033–1050. (discussion 1050–1094) (doi:10.1017/S0140525X01000127)
- 14 Mitchinson, B., Pearson, M., Pipe, T. & Prescott, T. J. 2011 In *Biomimetic robots as scientific models: a view from the whisker tip* (ed. J. Krichmar), Boston, MA: MIT Press.
- 15 Carvell, G. E. & Simons, D. J. 1990 Biometric analyses of vibrissal tactile discrimination in the rat. *J. Neurosci.* **10**, 2638–2648.
- 16 Prescott, T. J., Pearson, M. J., Mitchinson, B. & Pipe, T. 2009 Whisking with robots: from rat vibrissae to biomimetic technology for active touch. *IEEE Robot. Autom. Mag.* **16**, 42–50. (doi:10.1109/MRA.2009.933624)
- 17 Russell, R. A. 1985 Object recognition using articulated whisker probes. In *Int. Symp. on Industrial Robots*, pp. 605–612. Japan Industrial Robot Assoc.
- 18 Fend, M. 2005 Whisker based texture discrimination on a mobile robot. *Adv. Artif. Life* **3630**, 302–311. (doi:10.1007/11553090_31)
- 19 Solomon, J. H. & Hartmann, M. J. 2006 Robotic whiskers used to sense features. *Nature* **443**, 525. (doi:10.1038/443525a)
- 20 Kim, D. & Möller, R. 2007 Biomimetic whiskers for shape recognition. *Robot. Auton. Syst.* **55**, 229–243. (doi:10.1016/j.robot.2006.08.001)
- 21 Brecht, M., Preilowski, B. & Merzenich, M. M. 1997 Functional architecture of the mystacial vibrissae. *Behav. Brain Res.* **84**, 81–97. (doi:10.1016/S0166-4328(97)83328-1)
- 22 Towal, R. B., Quist, B. W., Gopal, V., Solomon, J. H. & Hartmann, M. J. Z. 2011 The morphology of the rat vibrissal array: a model for quantifying spatiotemporal patterns of whisker-object contact. *PLoS Comput. Biol.* **7**, 1–17. (doi:10.1371/journal.pcbi.1001120)
- 23 Hartmann, M. J., Johnson, N. J., Towal, R. B. & Assad, C. 2003 Mechanical characteristics of rat vibrissae: resonant frequencies and damping in isolated whiskers and in the awake behaving animal. *J. Neurosci.* **23**, 6510–6519.
- 24 Birdwell, J. A., Solomon, J. H., Thajchayapong, M., Taylor, M. A., Cheely, M., Towal, R. B., Conradt, J. & Hartmann, M. J. Z. 2007 Biomechanical models for radial distance determination by the rat vibrissal system. *J. Neurophysiol.* **98**, 2439–2455. (doi:10.1152/jn.00707.2006)
- 25 Pocock, R. I. 1914 On the facial vibrissae of Mammalia. *Proc. Zool. Soc. Lond.* **84**, 889–912
- 26 Haidarliu, S., Simony, E., Golomb, D. & Ahissar, E. 2011 Collagenous skeleton of the rat mystacial pad. *Anat. Rec. (Hoboken)* **294**, 764–773.
- 27 Hartmann, M. J. Z. 2011 A night in the life of a rat: vibrissal mechanics and tactile exploration. *Ann. N. Y. Acad. Sci.* **1225**, 110–118.
- 28 Williams, C. M. & Kramer, E. M. 2010 The advantages of a tapered whisker. *PLoS ONE* **5**, e8806. (doi:10.1371/journal.pone.0008806)
- 29 Ebara, S., Kumamoto, K., Matsuura, T., Mazurkiewicz, J. E. & Rice, F. L. 2002 Similarities and differences in the innervation of mystacial vibrissal follicle-sinus complexes in the rat and cat: a confocal microscopic study. *J. Comp. Neurol.* **449**, 103–119. (doi:10.1002/cne.10277)
- 30 Mitchinson, B., Gurney, K. N., Redgrave, P., Melhuish, C., Pipe, A. G., Pearson, M. J., Gilhespy, I. & Prescott, T. J. 2004 Empirically inspired simulated electro-mechanical model of the rat mystacial follicle-sinus complex. *Proc. R. Soc. Lond. B* **271**, 2509–2516. (doi:10.1098/rspb.2004.2882)
- 31 Jones, L. M., Lee, S., Trageser, J. C., Simons, D. J. & Keller, A. 2004 Precise temporal responses in whisker trigeminal neurons. *J. Neurophysiol.* **92**, 665–668. (doi:10.1152/jn.00031.2004)
- 32 Szwed, M., Bagdasarian, K. & Ahissar, E. 2003 Encoding of vibrissal active touch. *Neuron* **40**, 621–630. (doi:10.1016/S0896-6273(03)00671-8)
- 33 Haidarliu, S., Simony, E., Golomb, D. & Ahissar, E. 2010 Muscle architecture in the mystacial pad of the rat. *Anat. Rec. (Hoboken)* **293**, 1192–1206. (doi:10.1002/ar.21156)
- 34 Bermejo, R., Vyas, A. & Zeigler, H. P. 2002 Topography of rodent whisking—I. Two-dimensional monitoring of whisker movements. *Somatosens. Mot. Res.* **19**, 341–346. (doi:10.1080/0899022021000037809)
- 35 Knutsen, P. M., Biess, A. & Ahissar, E. 2008 Vibrissal kinematics in 3D: tight coupling of azimuth, elevation and torsion across different whisking modes. *Neuron* **59**, 35–42. (doi:10.1016/j.neuron.2008.05.013)
- 36 Grant, R. A., Mitchinson, B., Fox, C. & Prescott, T. J. 2009 Active touch sensing in the rat: anticipatory and regulatory control of whisker movements during surface exploration. *J. Neurophysiol.* **101**, 862–874. (doi:10.1152/jn.90783.2008)
- 37 Hill, D. N., Bermejo, R., Zeigler, H. P. & Kleinfeld, D. 2008 Biomechanics of the vibrissa motor plant in rat: rhythmic whisking consists of triphasic neuromuscular activity. *J. Neurosci.* **28**, 3438–3455. (doi:10.1523/JNEUROSCI.5008-07.2008)
- 38 Mitchinson, B., Martin, C. J., Grant, R. A. & Prescott, T. J. 2007 Feedback control in active sensing: rat exploratory whisking is modulated by environmental contact. *Proc. R. Soc. B* **274**, 1035–1041. (doi:10.1098/rspb.2006.0347)
- 39 Mitchinson, B. & Prescott, T. J. 2007 A computational model of whisking pattern generation. *Abstr. Somatosens. Motor Res.* **24**, 139–162.
- 40 Towal, R. B. & Hartmann, M. J. Z. 2008 Variability in velocity profiles during free-air whisking behavior of unrestrained rats. *J. Neurophysiol.* **100**, 740–752. (doi:10.1152/jn.01295.2007)
- 41 Pearson, M. J., Pipe, A. G., Melhuish, C., Mitchinson, B. & Prescott, T. J. 2007 Whiskerbot: a robotic active touch system modelled on the rat whisker sensory system. *Adapt. Behav.* **15**, 223–240. (doi:10.1177/1059712307082089)
- 42 Pearson, M. J., Mitchinson, B., Welsby, J., Pipe, T. & Prescott, T. J. 2010 SCRATCHbot: active tactile sensing in

- a whiskered mobile robot. In *Proc. 11th Int. Conf. on Simulation of adaptive behavior: from animals to animats*, pp. 93–103. Berlin, Germany: Springer.
- 43 Sullivan, J. C. *et al.* 2011 Tactile discrimination using active whisker sensors. *IEEE Sensors*.
- 44 Anderson, S. R., Pearson, M. J., Pipe, A., Prescott, T., Dean, P. & Porrill, J. 2010 Adaptive cancelation of self-generated sensory signals in a whisking robot. *Robot. IEEE Transact.* **26**, 1–12
- 45 Weber, R. C. 2007 *Robotino handbook 544305 DE/EN [User manual]*. Denkendorf, Germany: Festo Didactic GmbH.
- 46 Grant, R. A., Mitchinson, B. & Prescott, T. J. In press. The development of whisker control in rats in relation to locomotion. *Dev. Psychobiol.*
- 47 Lepora, N. F., Pearson, M. J., Mitchinson, B., Evans, M., Fox, C., Pipe, A. G., Gurney, K. & Prescott, T. J. 2010 Naive Bayes novelty detection for a moving, whiskered robot. In *IEEE Int. Conf. on Robotics and Biomimetics (ROBIO)*, pp. 131–136. IEEE.
- 48 Evans, M., Fox, C., Pearson, M. J., Lepora, N. F. & Prescott, T. J. 2010 Whisker-object contact speed affects radial distance estimation. In *IEEE Int. Conf. on Robotics and Biomimetics (ROBIO)*, pp. 720–725. IEEE.
- 49 Smith, A. M., Gosselin, G. & Houde, B. 2002 Deployment of fingertip forces in tactile exploration. *Exp. Brain Res.* **147**, 209–218. (doi:10.1007/s00221-002-1240-4)
- 50 Weiss, E. J. & Flanders, M. 2010 Somatosensory comparison during haptic tracing. *Cereb. Cortex.* **21**, 425–434. (doi:10.1093/cercor/bhq110)
- 51 Kleinfeld, D., Berg, R. W. & O'Connor, S. M. 1999 Anatomical loops and their electrical dynamics in relation to whisking by rat. *Somatosens. Mot. Res.* **16**, 69–88. (doi:10.1080/08990229970528)
- 52 Pietr, M. D., Knutsen, P. M., Shore, D. I., Ahissar, E. & Vogel, Z. 2010 Cannabinoids reveal separate controls for whisking amplitude and timing in rats. *J. Neurophysiol.* **104**, 2532–2542. (doi:10.1152/jn.01039.2009)